drones

MDPI

Article

Using UAV to Capture and Record Torrent Bed and Banks, Flood Debris, and Riparian Areas

Paschalis Koutalakis [1], Ourania Tzoraki [1], Giorgos Gkiatas [2] and George N. Zaimes [3,*]

[1] Department of Marine Sciences, University of the Aegean, 81100 Mytilene, Greece; koutalakis_p@yahoo.gr (P.K.); rania.tzoraki@aegean.gr (O.T.)
[2] Department of Forestry and Natural Environment, International Hellenic University, 1st km Drama-Mikrohoriou, 66100 Drama, Greece; george.giatas@hotmail.com
[3] UNESCO Chair Con-E-Ect, Department of Forestry and Natural Environment, International Hellenic University, 1st km Drama-Mikrohoriou, 66100 Drama, Greece
* Correspondence: zaimesg@for.ihu.gr; Tel.: +30-252-1060-416

Received: 11 November 2020; Accepted: 9 December 2020; Published: 14 December 2020

Abstract: Capturing and recording fluvio-geomorphological events is essential since these events can be very sudden and hazardous. Climate change is expected to increase flash floods intensity and frequency in the Mediterranean region, thus enhancing such events will also impact the adjacent riparian vegetation. The aim of this study was to capture and record the fluvial-geomorphological changes of the torrent bed and banks and flood debris events with the use of UAV images along a reach of Kallifytos torrent in northern Greece. In addition, a novel approach to detecting changes and assessing the conditions of the riparian vegetation was conducted by using UAV images that were validated with field data based on a visual protocol. Three flights were conducted using the DJI Spark UAV. Based on the images collected from these flights, orthomosaics were developed. The orthomosaics clearly identified changes in the torrent bed and detected debris flow events after major flood events. In addition, the results on the assessment of riparian vegetation conditions were satisfactory. Utilizing UAV images shows great potential to capture, record, and monitor fluvio-geomorphological events and riparian vegetation. Their utilization would help water managers to develop more sustainable management solutions based on actual field data.

Keywords: environmental status; fluvio-geomorphological events; granulometry; orthomosaics; stream; torrent; visual protocol

1. Introduction

Fluvio-geomorphological events can be very sudden and episodic [1], indicating that new innovative methods need to be utilized for their more effective recording and monitoring [2]. Of major interest are stream bed and stream bank changes and flood debris events as they can alter the channel flow path and cause major infrastructure failures. In the Mediterranean region, these are primarily caused by flash floods [3]. Flash floods are among the most dangerous natural disasters as they cause rapid torrential waters to flow in torrent and stream channels and cover the surrounding floodplains [4,5]. As flash floods are weather-related events (primarily the results of intense rainfall events), they are expected to be affected by climate change [6]. Specifically, their frequency and magnitude will be increased due to more extreme weather events caused by climate change such as extreme rainfall events [7,8]. One of the most vulnerable regions to climate change is the Mediterranean. In this region, the hydrological regime of intermittent streams and torrents is expected to become more extreme (higher peak flows but also no flow periods) due to the more intense rainfalls falling in shorter periods of time [9]. The frequency of larger flood events is expected to be increased

which should also intensify erosion and debris transport capacity [10,11]. Furthermore, these flood events will occur in watersheds with a drier Mediterranean environment (dry crusted soils and less vegetation cover due to greater droughts in magnitude and length), leading to more intense runoff and erosion phenomena [12,13]. Understanding the new hydrologic regime is necessary for the sustainable management of Mediterranean streams and torrents [14–16]. Excessive sediment as well as debris loading in streams and torrents have negative impacts on both the natural environment (water pollution, eutrophication, fish and wildlife losses) and the human/urban environment (health risk, failures in infrastructures, increased costs) [17,18]. The impacts of climate change on floods and erosion along with the increase in population and the infrastructure densification will also result in increased risk in regard to economic and human life losses [18–21].

Riparian areas can act as buffer zones that slow down surface runoff and trap sediments and other pollutants that originate from agricultural and urban activities, decrease stream velocities, and consequently reduce flood magnitudes [1,7,22–24]. One of the reasons why they can offer these ecosystem services is because of their location that is adjacent to streams (perennial, intermittent, and ephemeral), lakes, ponds, and estuarine–marine shorelines [25–27]. Riparian areas connect the surface and subsurface waterbodies with their adjacent uplands and are the transition zones between the terrestrial and aquatic ecosystem [28–31]. At the same time, the woody vegetation of the riparian areas, when not properly managed, can become woody debris (branches and tree trunks) during high flow conditions and/or flash floods [32,33]. Flash floods can carry significant amounts of sediments, rocks, and woody vegetation or even entire trees causing serious problems to human infrastructures [34]. The bedload material in gravel-bed channels is typical pebble and cobble interstratified with laminated gravel or coarse sand to boulder size material with significant damage potential [35].

Studying and understanding water erosion is a priority worldwide. [36]. In order to enhance our understanding and monitoring of the erosional process, a number of different methods have been developed and are being used. The most common and widely utilized method is the universal soil loss equation (USLE), a soil erosion model that predicts the rate of soil loss on a field slope, based on rainfall, soil type, slope, crops systems, land cover, and erosion control practices [37,38]. Additional methods to better record and indicate geomorphological changes, include traditional runoff plots [39], telemetric data loggers (data acquisition system) with ultrasonic signal erosion tools [2,40] and remote sensing tools utilizing unmanned aerial vehicles (UAVs) [41–43]. UAVs applications have grown rapidly during the last decade which include the scientific field of disaster management such as floods, erosion, earthquakes/landslides, and wildfires [44–50]. Zwęgliński [51] proved that UAV products (e.g., three-dimensional models and orthophoto maps) are applicable in sudden natural disasters and will become a necessity for all aerial disaster-related needs and damage reconnaissance. Finally, the recording and monitoring of fluvial geomorphology could be further enhanced by properly trained citizen scientists and could capture real-time geo-tagged photographs based on smartphones equipped with cameras and global positioning systems (GPS) [52].

The objective of this study was to assess, with the use of UAV images, the capturing and recoding of fluvio-geomorphological events such as erosion, deposition, and flood debris. The selected study area was located in Drama, a city in Greece, which has been affected during the last decades by a population increase while the urban sprawl consists mainly by grey infrastructure. In addition, the condition of the riparian areas was assessed using a visual protocol derived from UAV images in combination with field measurements. These previous assessments were conducted along a reach of a typical Mediterranean ephemeral stream (e.g., a torrent). The geomorphological condition of the torrent and its riparian zone were generated, by using airborne images and combined with field observation to validate the outputs. Using such images can enhance the accuracy of the measurements and evaluation of the impacts of the fluvio-geomorphological events. Land managers could utilize this new method to improve the recording of these fluvio-geomorphological phenomena. Improving the recording will help identify and select best management practices to mitigate the impact of such

events by implementing more sustainable and environmentally-friendly methods such as nature-based solutions and ecosystem-based approaches.

2. Materials and Methods

2.1. Study Torrent Reach

The study reach is located in Drama; a city in northern Greece built on the southern foothills of Falakro Mountain at an elevation of 114 m (Figure 1). The name of the city originates from the Greek word "idor" which means water and refers to the rich water supplies of the area [53,54]. The springs of Agia Barbara, along with its recreational park, the traditional old buildings, and watermills, form a combination of a natural wetland (shallow lakes and streams) and riparian environment within an urbanized area [27,55]. The torrent of Kallifytos (the studied torrent) has a direction from east to west that eventually discharges to the Agia Barbara stream. The torrent has a wide bed in all its length while it crosses and divides the city of Drama from its southern suburbs. In the recent decades, the urban sprawl of the city has decreased its physical environment and width (Figures 2 and 3). The natural torrent channel today disappears as an underground drainage canal that was constructed at the point it enters the urban environment. The top part of the underground canal is covered by roads, buildings, parks, parking, and other facilities [27]. The research in this study focuses on the sub-urban part of the Kallifytos torrent (east of the city) (Lat. 41°8′48.29″ N and Long. 24°10′19.85″ E), a typical ephemeral Greek torrent that has flash flood risk potential after heavy rainfalls. Ephemeral streams (e.g., torrents) are the most common running water bodies in southern Europe [3]. Their flow can change in hours from no flow to a flow with great rapidity and carrying large amounts of water, sediments, and debris [56]. The studied torrent should be monitored due to its proximity to Drama City and its frequent flooding of the road network and bridge. The torrent has transported and deposited large amounts of sediment and debris and altered the channel and bed shape in the past, during and after heavy rainfalls. In the studied reach, the torrent crosses an Irish bridge (length: 45 m and width: 8 m) with 30 culverts of concrete pipes (diameter: 0.80 m and width: 8 m).

Figure 1. The study area in Drama (yellow triangle) located in Greece (Source: Esri, DigitalGlobe, GeoEye, EarthStar Geographics. CNES/Airbus DS, USDA, USGS, AeroGRID, IGN, and the GIS Users Community).

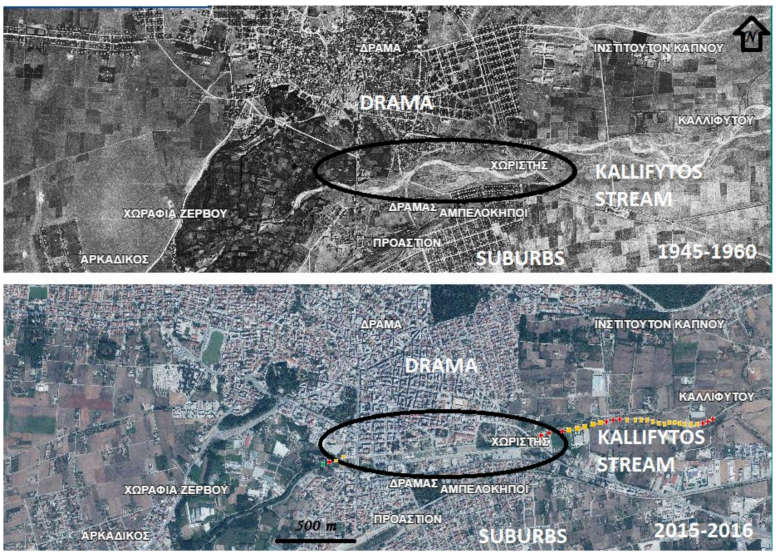

Figure 2. Satellite images illustrating the difference of the urban areas and the alteration of Kallifytos torrent due to urban sprawl. The images are from 1945–1960 (above) and 2015–2016 (below). The natural torrent bed (in the past) and the underground drainage channel (now) are depicted inside the black area (Source: KTIMATOLOGIO SA). Additionally, field measurements depict in different color the environmental status of the torrent (red is poor, yellow is moderate, and green is good) based on an optical protocol.

2.2. *Airborne and Field Measurements*

The DJI Spark UAV (Shenzhen, China) was selected to capture the ortho-images. The manually grid flight plan captured frequent intersected images. The DJI Spark is a mini drone (143 × 143 mm) and its weight is only 300 g [57]. It has a GPS/GLONASS, as a satellite positioning system, while its 1/2.3" CMOS camera captures Full HD 1080p video and 3968 × 2976 pixels of image resolution [58]. Airborne and field measurements were taken during three different dates (Figure 4):

(i) 1st flight—31 January 2020 (black area). This flight focused on the area starting upstream from the bridge and covering the upland bed. This flight lasted 20 min and captured 97 images. Based on the images of this flight, emphasis was given to recording and showcasing the newly formed torrent bed and flow paths. The day before the flight high flows passed through the torrent.

(ii) 2nd flight—7 August 2020 (red area). This flight targeted the area surrounding the bridge. It lasted 10 min and captured 60 images. These images allowed to record flow paths, debris material, torrent bed substrate, and geomorphological and riparian vegetation changes.

(iii) 3rd flight—19 September 2020 (yellow area). This final flight included a wider area of both sides of the banks of the bridge. This flight lasted 25 min and captured 196 images. Based on this flight, the torrent bank floodplain and riparian zone were delineated. In addition, the images of this flight were compared to the images of the 2nd flight to assess geomorphological and riparian vegetation changes.

Figure 3. Google images illustrating the alteration of Kallifytos torrent due to the increase of urban infrastructure and intervention in the torrent and entire area. The images are from 2004 (top photo) and 2020 (bottom photo) (Source: Google Earth).

The orthomosaics, produced by photogrammetry based on the UAV images, allowed us to measure different spatial characteristics. The spatial characteristics such as the perimeter and the area of different geomorphological areas (riparian area, floodplain, channel, torrent banks, and main flow path) were digitized and recorded. In addition, airborne images were helpful to provide additional easy and quick measurements or information such as granulometry of the riverbed material, vegetated areas, and flood debris, as well as truck tracks.

During these flights, the DJI spark hovered at 50 m above the ground. The manually grid flight plans covered the study area and captured the images. Ground control points (GCPs) are a necessity for UAV topographic surveys in order to geo-reference the images [59]. The GCPs can be measured in the field by using a GNSS receiver to store the coordinates or by utilizing direct geo-referencing using a UAV mounted GNSS antenna and no GCPs [60]. The GPS-GNSS JAVAD TRIUMPH-1 receiver (San Jose, USA) was used to include twenty GCPs either as physical spots (e.g., trees, rocks) or human constructions (waste water treatment plant) and artificial marks (e.g., topographic milestones and targets). The GCPs were used to ensure the geospatial accuracy of the imagery rated at 1 cm accuracy. Furthermore, field measurements included cross sections measurements and the use of topographic milestones in order to capture the dimensions of the under-bridge culverts. Finally, another visit on 12 October 2020 was necessary as a supplementary day of field measurements to illustrate the recent conditions in the torrent geomorphology after a heavy rainfall event.

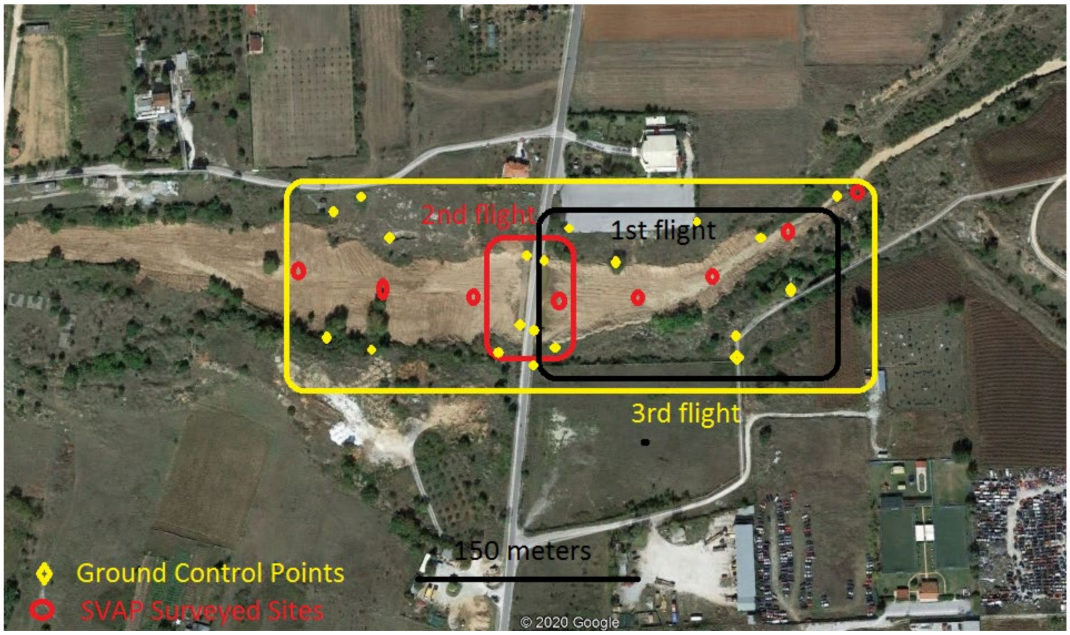

Figure 4. The areas covered by the three unmanned aerial vehicles (UAV) flights. The 1st flight in 31 January 2020 is in the black area, the 2nd flight is in the red area, and the 3rd flight is in the yellow one (Source: Google Earth). In addition, the 20 ground control points (GCPs) are depicted in yellow diamonds and the 8 surveyed sites for the optical protocol in red circles.

2.3. Software for the Analyis of the UAV Images

The Agisoft Metashape, formerly known as PhotoScan, is a professional commercial tool developed for photogrammetry by Agisoft LLC (St. Petersburg, Russia) [61]. The software is able to combine the digital images in order to generate geo-referenced 3D models, aerial triangulation, polygonal models (plain/textured), DSMs, and orthomosaics [62]. The user has to select the initial images while the following processing is a fully automated workflow and enables a non-specialist to get familiar with it very quickly and easily. At least two different images that have common points are requested in order to reconstruct the studied area [63]. Images can be captured from any position. The images are geo-referenced images due to the onboard GPS coordinates attached to each image but high-accuracy control reference points can be additionally used in the bundle adjustment to further enhance the accuracy of the positioned orthomosaics and 3D models [64]. The utilized hardware was an ACER Aspire 64-bit (New Taipei, Taiwan) which has a 4 GB RAM, Intel Core i3-4000M processor 2.40 GHz, Nvidia GeForce 840M, and an SSD disk. The images were combined to produce the point clouds and finally the three orthomosaics of the studied reach. The first flight generated the orthomosaic (Figure 5) based on 97 images. The second flight was focused on the bridge, so only 46 images were used to produce the orthomosaic of the area (Figure 6a) and the digital elevation model (DEM) (Figure 7a). The third flight captured 196 images and created another orthomosaic (Figure 6b). The produced maps were further analyzed in ESRI ArcGIS 10.4. (Redlands, California, USA).

2.4. Stream Visual Assessment Protocol (SVAP)—Field and Image Assessments

The SVAP is a visual protocol that addresses the environmental status of streams or torrents and its riparian areas [65,66]. It was developed by the Natural Resources Conservation Service United States Department of Agriculture (USDA-NRCS). The protocol, firstly, gathers general information on the site surveyed and follows with the detailed information on the stream or torrent and the riparian characteristics [67]. Specifically, fourteen characteristics are evaluated and these selected characteristics and their values have been adjusted to the Greek and Mediterranean natural environmental conditions [68]. The evaluated characteristics are: (i) channel condition, (ii) hydrologic

alteration, (iii) riparian zone condition, (iv) bank stability, (v) water existence, (vi) water appearance, (vii) livestock shed presence, (viii) instream fish cover, (ix) pools, (x) insect/invertebrate habitat, (xi) canopy cover, (xii) manure presence, (xiii) biological wastewater treatment presence, and (xiv) garbage presence [69]. The values of these characteristics can range from 1–10, while the final score for a surveyed site is the average of these 14 characteristics. Based on the values of the 14 characteristics, the SVAP has 4 categories that represent the stream or torrent and riparian area environmental condition. These are: (A) Poor condition with mean values less than 6, (B) Moderate condition with mean values ranging from 6.1 to 7.4, (C) Good condition with mean values ranging from 7.5 to 8.9, and (D) Excellent condition with mean values greater than 9 [70]. In this study, the SVAP rating was performed based on the recorded airborne data, in addition to the field observation of the mentioned characteristics. Thirty equidistant sites were surveyed based on the field measurements starting downstream from the bridge that our study focused on and continuing upstream. The first eight sites surveyed were upstream from the Irish bride while the rest were downstream. Eight of these sites were surveyed based on the airborne images and compared to the visual protocol field measurements to validate the effectiveness of the airborne images to perform such a visual assessment.

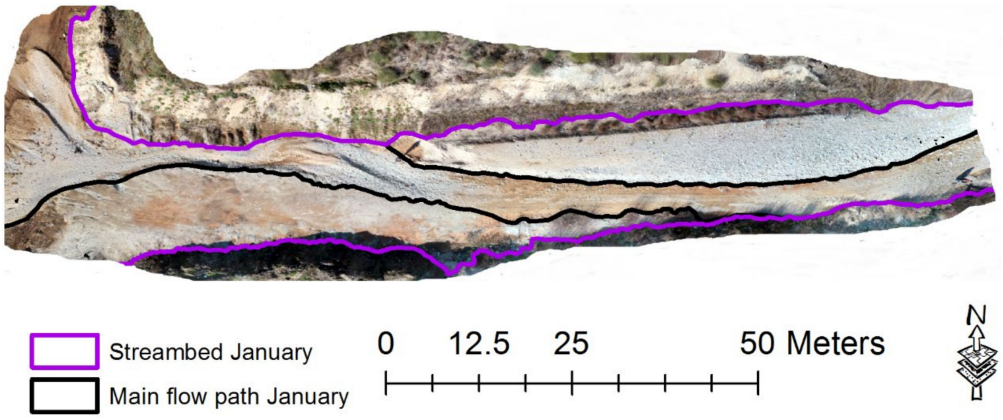

Figure 5. The orthomosaic of the study area based on the flight on 31 January 2020. The torrent bed boundary is within the purple line and the main water flow path boundary (thalweg) is within the black line.

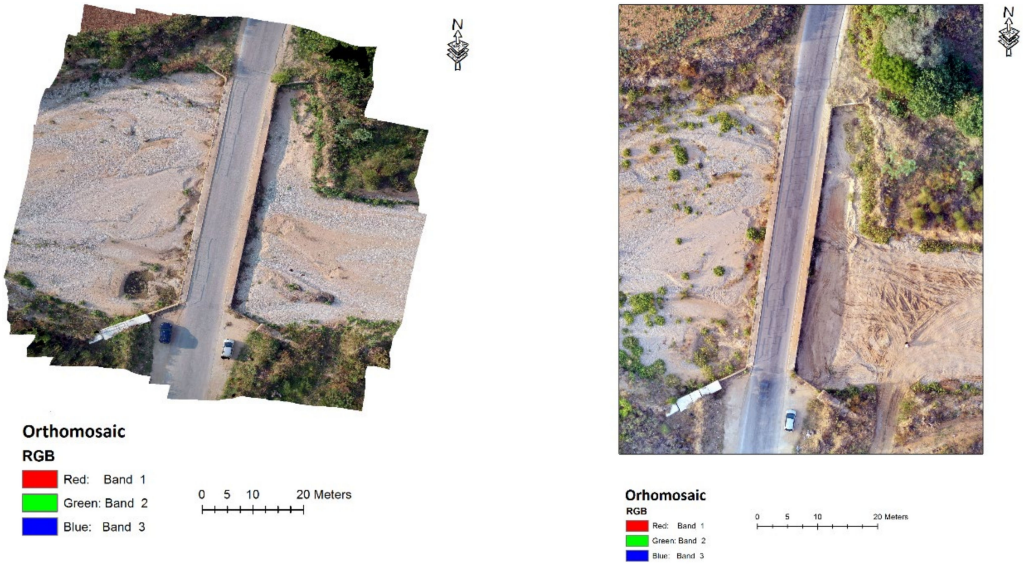

(**a**) (**b**)

Figure 6. The orthomosaic of the study area based on the flight of (**a**) 7 August 2020 and (**b**) 19 September 2020.

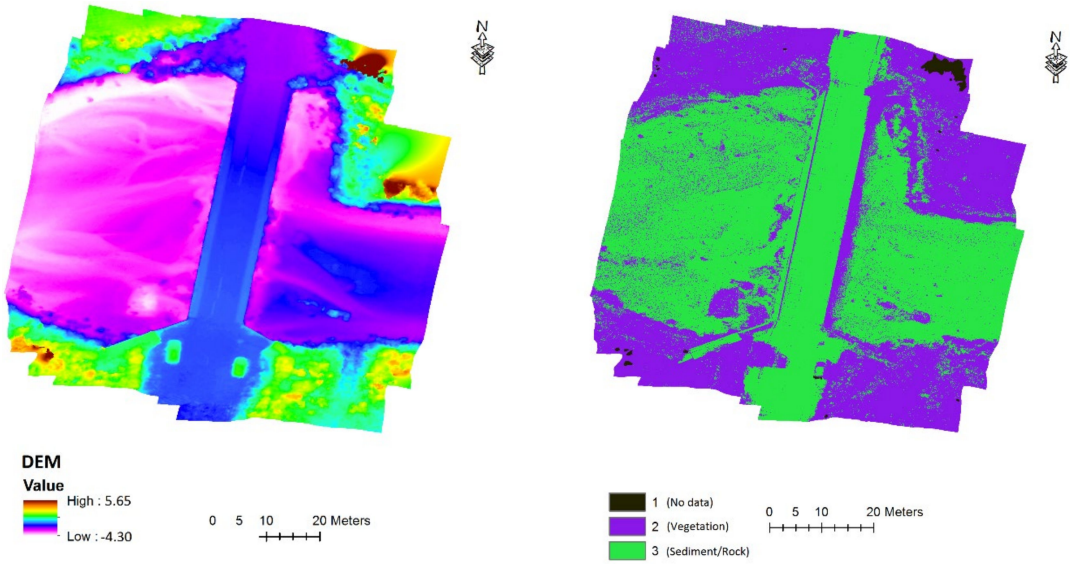

(**a**) (**b**)

Figure 7. (**a**) The digital elevation model (DEM) of the study area developed based on the flight of 7 August 2020, the legend illustrates the elevation; (**b**) The elevation distributed in three categories in order to showcase the vegetated areas: (1) no data (black), (2) vegetation (purple), and (3) sediment/rock (green).

3. Results

3.1. 1st Flight—Showcasing the Torrent Bed and Flow Paths

The orthomosaic produced by the images captured on 31 January 2020 is presented in Figure 5. Unfortunately, it was impossible to capture the bridge due to a malfunction of the restriction zones during the drone flight. As a result, the orthomosaic depicts the stream bed from the right side of the bridge (upstream). This orthophoto was inserted in ArcGIS in order to digitize the torrent bed area, but also the main water flow path that was created during the previous days' high flow event. The orthomosaic highlights the main water flow path (probably the thalweg) inside the main channel. The elevation difference between the main flow path and the surrounding torrent bed ranged from 1 to 22 cm. The entire torrent bed area is surrounded by the purple line, while the boundary of the main water path is within the black lines. This main flow path is where water runs through during low flow events. The black lines join the purple at the top boundary in the left part that is common for both areas. The difference of the width was significant from 3.1 to 14.3 m for the main flow path to the main channel respectively. The perimeter of the streambed area was equal to 385.0 m and the area was 3029.9 m^2 (within the purple lines). In addition, the perimeter of the main flow path was 370.8 m, while its area was 1280.0 m^2 (within the black lines).

3.2. 2nd Flight—Flow Paths, Flood Debris, Riparian Vegetation, and Torrent Bed Substrate

The DEM was also produced based on the orthomosaic for the August flight (7 August 2020). The DEM (Figure 7a) has its zero level at the bridge top and this is the reason why minus values (-) are also present in the image that represent the torrent bed. The flow paths are visible due to the height variance. Three main flow paths that start from the right part under the bridge culverts and continue at the left section mainly at the top of the image. This is a result of the debris and sediment deposition at the central part of the bridge at the right section which forces the main body of water to the right bank (top of the image). Furthermore, we were able to produce a map (Figure 7b) that categorizes the different illustrations mainly based on the vegetation and creates the following categories: (1) no data (black), (2) vegetation (purple), and (3) sediment/rock (green). This map highlights the vegetation

in front of the bridge culverts adjusted at the right section of the bridge. The riparian vegetation consists mainly by low vegetation and trees: *Morus ssp.*, *Ailanthus altissima*, *Avena sativa*, *Melissa officinalis*, *Populus nigra*, *Salix alba*, *Onopordum acanthium*, and *Arctium* ssp. among others. The dead vegetation material represents the debris that act as barrier and have a negative impact, enhancing the potential and creating floods (Figure 8). Debris material are mainly tree brunches but also large rocks. Their dimensions can be measured by the recorded airborne images or by normal field monitoring (Figure 9). A granulometric analysis was also performed on the orthomosaics via ArcGIS. The airborne measurements were verified by using past field measurements. Specifically, field measurements, by using a tape measure, were collected along five cross sections downstream from the bridge. For the bed material, the pebbles and cobbles were measured in the two dimensions (largest and smallest). The majority of the material ranged from 1 to 20 cm (84.5%) and 1 to 10 cm (85.1%), concerning length and width, respectively. The results between field and airborne measurements were very similar in their dimensions in both cases which ranged from 1–67 cm. This highlights that UAV images can be utilized as an innovative, quick, and easy-to-use method to perform granulometry on these types of torrents.

(**a**) (**b**)

Figure 8. (**a**) The debris (tree brunches and other material) are depicted in the right section of the bridge; (**b**) A rare clean culvert under the bridge.

(**a**) (**b**)

Figure 9. The bed material transported by the water flow during the torrential phenomena (**a**) performing granulometric field measurements; (**b**) The bed material captured by the drone flight.

3.3. 3rd Flight—Torrent Banks, Floodplain and Riparian Zone Delineation

The 3rd airborne monitoring was conducted during September 2020 to illustrate possible change in the torrent bed due to the removal of the bed material and debris by excavators and trucks that belong to the municipality of Drama. The generated orthomosaic is depicted in Figure 10 based on this 3rd flight while Figure 6b is the same flight focused at the bridge for comparison purposes. The digitization in ArcGIS resulted in the boundaries of the riparian vegetation area (green lines), floodplain boundaries (red lines), and torrent bank boundaries (blue lines). We differentiated the last two based on the bank elevation that ranged from 0.8 to 2.70 m, but also the presence and absence of vegetation. The width of the riparian area ranged from 46.6 to 96.7 m. The floodplain and bed area did not cover the same area, although in some locations, the boundaries were the same, and as a result, the width ranges were identical from 5.6 to 58.8 m. The riparian perimeter was equal to 531.6 m and its area was 17091.5 m^2. The floodplain perimeter was calculated as 456.4 m, while its area as 4444.8 m^2. Finally, the stream bed perimeter equals to 441.1 m and the area is measured as 3936.1 m^2.

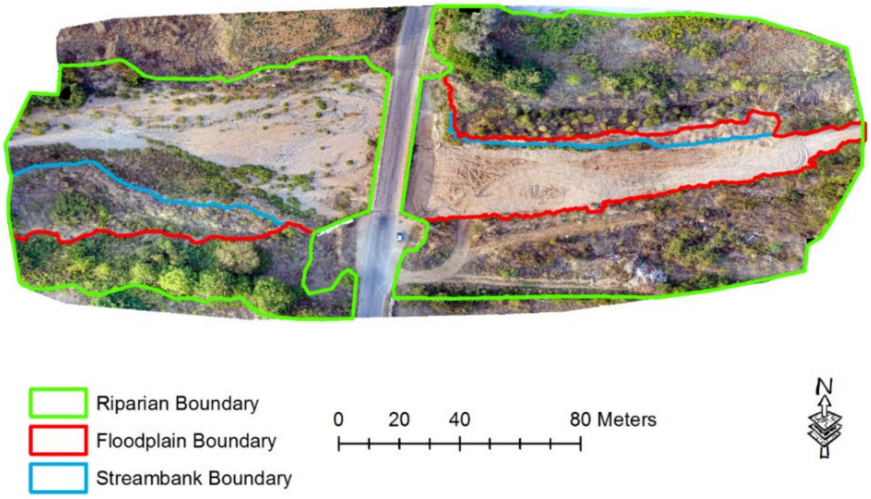

Figure 10. The orthomosaic of the study area based on the flight of 19 September 2020. The torrent bank areas (blue lines), the floodplain area (red lines), and the riparian vegetation area (green lines) were digitized to showcase their difference.

3.4. 2nd and 3rd Flights—Geomorphological and Riparian Vegetation Changes

The flight in August 2020 produced the orthomosaic focused on the bridge (Figure 6a). The measurements were taken to record the changes due the flood phenomena during this period, which resulted in large amounts of sediment and debris transported and deposited. In addition, a part of the orthomosaic captured in September 2020 was compared to the previous in regards to bed changes (Figure 6b). The truck tracks were clearly recorded in the 3rd flight which recorded the additional bed material (from the flood events recorded in the August flight) at the right section of the bridge. The rest of the torrent bed, especially at the left section of the bridge, remained relatively the same in both flights. Another substantial difference were the changes in the riparian vegetation on the banks. The difference was because of the hot summer before the 7 August 2020 flight, while before the 19 September 2020 flight, the shrub vegetation was substantially denser in the left section.

3.5. 1st and 3rd Flights—SVAP Field and UAV Results—Torrent Conditions

The results based on SVAP field measurements are not very encouraging for the environmental condition of the torrent and its riparian area (Table 1). Out of the 30 surveyed sites, 1/3 are in poor condition. In addition, only one is in good condition and none in excellent. The site in good condition was the furthest away from the starting point, which was the Irish bridge. Overall, most sites are in moderate conditions. Figure 2 depicts in different color (poor is red, moderate is yellow, and good

is green) the environmental condition of the surveyed sites based on SVAP field measurements. The environmental conditions of the torrent and its riparian area need to be improved. Based on individual characteristics, the canopy cover has low values, indicating that the riparian vegetation is limited and is not providing the entire potential spectrum of its ecosystem services. The lack of canopy cover is also impacting stream bank stability, which also has low values in many sites, indicating that erosional and depositional processes are prevalent in this studied torrent. In contrast, the absence of the canopy cover enabled us to generate the specific environmental assessment also via airborne monitoring. The images captured by the UAV were in high resolution and covered the necessary spatial extent in order to record all 14 characteristics. The values of the SVAP characteristics between the airborne images and the field measurements in the eight compared cross-sections differed 1–2 out of a scale 1–10. These results are very encouraging. More specifically, the water-related characteristics with both ways did not receive values, something that was expected. Kallifytos torrent hydrologic regime is ephemeral as water flow is observed only after heavy rainfall events. The UAV images allowed the identification of most of the other characteristics because of the limited canopy cover that existed in the area. Channel condition, hydrologic alteration, riparian zone condition, bank stability, water existence, water appearance, pools, livestock shed presence, biological wastewater treatment presence, and garbage presence were easily obtained due to the conditions of the pilot area and resolution of the images. To recognize the manure presence on the banks and bed with UAV images was impossible. Instead, we concentrated on identifying the narrow livestock paths in the riparian zone which started from the nearby livestock units and ended in on near the torrent channel. Stream fish cover was difficult to identify although the images allowed to see certain characteristics such as vegetation overhang, bank undercutting, etc. Insect/invertebrate habitat is also a difficult characteristic to be recorded in the images, but flying insects can be spotted during flights and some of the habitat characteristics can be spotted similarly to fish cover. Finally, detecting biological wastewater treatment is possible, since the drone can cover large areas and lengths of the torrent addressed.

Table 1. The 14 characteristics used in Stream Visual Assessment Protocol (SVAP) index, for the overall rating of the quality of the site based on the filed measurements.

C.S. [1]	i	ii	iii	iv	v	vi	vii	viii	ix	x	xi	xii	xiii	xiv	M	C
1	2	9	5	2	-	-	5	-	-	9	1	1	1	3	3.8	Poor
2	1	9	9	4	-	-	5	-	-	9	1	3	1	9	5.1	Poor
3	6	9	9	6	-	-	4	-	-	9	2	4	1	9	5.9	Poor
4	9	10	10	9	-	-	9	-	-	9	1	2	1	10	7.0	Moderate
5	7	9	10	7	-	-	9	-	-	9	1	3	1	9	6.5	Moderate
6	9	9	10	9	-	-	9	-	-	9	2	3	1	10	7.1	Moderate
7	9	9	10	10	-	-	9	-	-	9	2	7	1	9	7.5	Moderate
8	9	10	9	6	-	-	9	-	-	9	1	9	1	9	7.2	Moderate
9	9	10	10	7	-	-	9	-	-	9	1	9	1	10	7.5	Moderate
10	4	9	9	10	-	-	10	-	-	9	1	9	1	8	7.0	Moderate
11	9	9	10	8	-	-	9	-	-	10	1	10	1	7	7.4	Moderate
12	7	10	10	9	-	-	10	-	-	10	2	4	1	10	7.3	Moderate
13	10	10	9	8	-	-	9	-	-	10	1	9	1	7	7.4	Moderate
14	10	9	10	9	-	-	9	-	-	9	5	5	1	6	7.3	Moderate
15	10	9	10	7	2	10	9	1	1	10	1	10	1	10	6.5	Moderate
16	5	9	9	8	2	8	10	1	2	10	2	10	1	7	6.0	Poor
17	9	9	5	5	4	6	9	2	4	7	2	8	1	3	5.3	Poor
18	4	9	8	7	-	-	9	-	-	7	2	6	1	3	5.6	Poor
19	5	9	4	7	-	-	9	-	-	8	1	10	1	8	6.2	Moderate
20	5	9	5	7	-	-	9	-	-	10	1	10	1	8	6.6	Moderate
21	5	10	5	7	-	-	10	-	-	9	1	8	1	8	6.9	Moderate
22	5	10	8	10	-	-	9	-	-	8	0	5	1	7	6.3	Moderate
23	5	10	8	8	-	-	10	-	-	7	5	10	1	10	6.8	Moderate
24	5	2	8	8	1	2	9	9	2	10	5	10	1	7	5.5	Poor
25	5	9	8	5	-	-	10	0	0	8	5	9	1	8	5.0	Poor

Table 1. *Cont.*

C.S. [1]	i	ii	iii	iv	v	vi	vii	viii	ix	x	xi	xii	xiii	xiv	M	C
26	10	9	9	5	-	-	9	0	0	8	5	4	1	3	4.5	Poor
27	10	9	10	9	8	1	9	4	7	10	5	9	1	1	6.6	Moderate
28	10	9	10	5	7	1	9	10	5	10	8	9	1	5	7.1	Moderate
29	10	9	9	5	2	1	9	4	1	7	2	10	1	8	5.6	Poor
30	10	9	10	8	3	9	10	2	5	10	9	10	1	10	7.6	Good

[1] C.S.: Cross section number, (i) channel condition, (ii) hydrologic alteration, (iii) riparian zone condition, (iv) bank stability, (v) water existence, (vi) water appearance, (vii) livestock shed presence, (viii) instream fish cover, (ix) pools, (x) insect/ invertebrate habitat, (xi) canopy cover, (xii) manure presence, (xiii) biological wastewater treatment existence, (xiv) garbage presence, M mean value, C: condition.

4. Discussion

A large percentage of the global river network is composed of temporary waterways, especially in semi-arid and arid regions [71]. Temporary streams (torrents) dominate the hydrographic network of Greece, while their watershed area covers approximately 42.5% of the total area of Greece [72]. The no flow periods of temporary streams like Kallifytos torrent are expected to increase due to climate change impacts and increased water demands [73,74]. In addition, climate change scenarios expect higher surface runoff volumes and peaks that would lead to increased fluvio-geomorphological events and sediment and debris loadings transportation capacity in torrents [8,75]. Furthermore, UAVs' products and photogrammetric tools have already proven their potential use in many scientific fields, including the geomorphological monitoring of rivers, streams, and torrents [76–79].

The specific study focused on the reach of the Kallifytos torrent in northern Greece, a typical Mediterranean ephemeral stream that carries large amounts of sediment and debris after high precipitation events and this results in severe flood phenomena. This torrent has a moderate to poor quality based on the SVAP index results. Only one site was in good conditions (based on the field measurements) and none in excellent. This should be a concern since its riparian areas are not able to offer their ecosystem services to their full extent. In many cases, especially when the conditions were bad, minimal ecosystem services are provided. Some of the ecosystem services offered by riparian areas that are in excellent conditions include increased infiltration capacity and aquifer recharge, increased stream bank stability, reduced surface erosion and sediment transport and loading in water bodies, decreased flood magnitudes, and enhanced flood waters storage [10,80]. This is why it was not surprising that the SVAP recorded many unstable stream banks and low vegetation cover. Stream channels with minimal or degraded riparian vegetation are more active geomorphologically, leading to many changes that were recorded by the drone's flights. Overall, the assessment of the visual protocol via airborne measurements, produced good results when compared to the field measurements. This is an innovation of the study that can be applied widely in such a type of torrent (with limited vegetation cover) in a fast and user-friendly way. Further testing of the applicability of the visual protocol by utilizing UAV images is being conducted by the authors in order to adapt it to different types of Greek streams (ephemeral, intermittent, and perennial).

The produced orthomosaics, based on the images collected from the three flights, were inserted in ArcGIS in order to digitize the boundaries of the different geomorphological areas of the specific reach of the torrent. This allowed to easily capture and measure morphometric data such as perimeter and area. The focus was on the riparian area, the floodplain, and the channel of the torrent, but also the main flow paths. Substantial changes in riparian vegetation were recorded due to the hot summer before the 7 August 2020 flight, while before the 19 September 2020 flight, the shrub vegetation was substantially denser in the left section. This is probably due to the flood events that increase the soil moisture and water table levels, thus providing immediate water sources for the riparian vegetation. Overall, the orthomosaics can help water managers to better record geomorphological changes in the future if more frequent flights are taken.

The orthomosaics enable us to compare the dimensions among different geomorphological characteristics of the torrent. The floodplain is the area of land adjacent to a stream, river, torrent,

thus frequently covering a greater area than the streambed, as in the case [81,82]. The main flow path (thalweg) is characterized by the lowest points along the entire streambed [83] and while its morphology can vary even during the year, it is always less or identical to the area covered by the streambed [84]. Additionally, riparian areas as buffer zones include the adjacent terrestrial areas that are influenced by the aquatic ecosystem. The extent of a riparian area into the terrestrial environment is highly correlated to the water and can be identified by the morphology, geology, and vegetation [85]. While the riparian area can be associated and be similar to the floodplain [86], in some cases, it may differ in dimensions. In our case, the floodplain area is less than the riparian area because of the channel morphology and the riparian vegetation width that is affected by the groundwater to a greater extent than the flooded areas. The floodplain area was 74% less than the riparian area and 11.4% greater than the streambed. Subsequently, the streambed area represented 23% of the riparian area. Additionally, the main flow path was 42.2% of the streambed area based on the specific orthomosaics in the described three different flight days.

Granulometry via UAVs photogrammetry is a promising alternative in comparison to field gravel dimensions measurements by using a type measure and sampling gravels in squared sections located in floodplains [87,88]. In addition, UAV-based products can be better than other remote sensing approaches for grain size quantification because of the great accuracy and resolution of the images [89]. Although, granules are three-dimensional objects for which at least three parameters (length, width, and height) are required for a complete description [90], still the orthomosaics could not provide the height data, so only the two dimensions (length and width) were enough to compare the field data with the airborne results. The dimensions can be measured very quickly via this methodology and can cover a greater area in contrast to field-based measurements that are more time-consuming. Furthermore, the orthomosaics were able to identify the vegetation debris that blocked the culverts under the Irish bridge. This was done by the produced DEM of the area and the further segregation of the vegetation cover from the sediment/rock material. The DEM can be helpful in many ways and different approaches in regard to environmental sciences [91–93]. For the needs of this study, the importance lies in determining the torrent flow paths and the locations where the debris created barriers. This would help water managers make proper management plans to stop these materials from reaching the central part of the bridge, as it was recorded by the drone flights.

In addition, orthomosaics showcased the changes on the torrent bed because of human intervention. The removal of bed material and debris by excavators and trucks is a common practice in Greece to "clean" the torrent bed from this additional material that is carried and deposited by flash flood events. This "cleaning" method has many negative effects in the fluvial environment due to human alteration of the torrent bed, the changes in the geomorphology or even the hydraulic conditions, the degradation of the riparian vegetation, the destruction of habitats environment, and the fatality of micro-invertebrates or other animals that exist in the torrent bed during these works. Furthermore, the specific case study showcases that only the bed material removal was achieved, while the debris remain and continued to block the culverts (the most serious problem) of the Irish bridge, resulting to the repeated same flood phenomena (Figure 11). The solutions to such problems should include more environmentally friendly methods such as ecosystem-based approaches and nature-based solutions to reduce flows and sediment transport capacity [94]. Unfortunately, in most urban cases, the riparian areas are completely cemented and the natural riparian vegetation is devoid, which does not provide a long-term sustainable solution [27].

(**a**) (**b**)

Figure 11. (**a**) Showing the flood phenomena at the right section of the bridge/torrent; (**b**) Upstream from the bridge the truck tracks are clearly evident. Images captured 13 October 2020.

5. Conclusions

The utilization of new technologies can enhance the recording and monitoring of fluvio-geomorphological and riparian changes, thus leading to more effective management plans. Based on UAV images, the flow paths, torrent bed and banks, floodplains, and riparian vegetation were delineated. In addition, the condition of the riparian vegetation, the recording of debris material, and the identification of seasonal riparian vegetation changes were accomplished. Implementing the SVAP based on UAV images appears to produce good results in comparison to the field measurements, and is a promising tool to rate the riparian conditions. The recorded previously mentioned parameters can help water managers develop science-based plans for the sustainable management of torrents. This is necessary since it is expected that their hydrologic regime will become more extreme due to climate with more frequent and higher magnitude flash floods and longer periods of drought with no flow. Compared to field measurements, UAV images can be more time efficient, although some field measurements will still be required for validation purposes. Still, the usefulness of this method will depend on obtaining the necessary flight permissions, the proximity to the area, the absence of nearby buildings or other obstacles, and the lack of canopy cover that impact the quality of the captured images.

Author Contributions: Conceptualization and Methodology, P.K.; O.T. and G.N.Z.; Literature Review, P.K. G.N.Z. and G.G.; Field Measurements and Software Application, P.K. and G.G.; Data Analysis, Visualization and Validation, P.K.; G.N.Z. and G.G.; Writing—Original Draft Preparation, P.K. and G.N.Z.; Writing—Review & Editing, O.T. and G.N.Z. All authors have read and agreed to the published version of the manuscript.

Funding: This research received no external funding.

Conflicts of Interest: The authors declare no conflict of interest.

References

1. Zaimes, G.N.; Tufekcioglu, M.; Schultz, R.C. Riparian land-use impacts on stream bank and gully erosion in agricultural watersheds: What we have learned. *Water* **2019**, *11*, 1343. [CrossRef]
2. Zaimes, G.N.; Ioannou, K.; Iakovoglou, V.; Kosmadakis, I.; Koutalakis, P.; Ranis, G.; Emmanouloudis, D.; Schultz, R.C. Improving soil erosion prevention in Greece with new tools. *J. Eng. Sci. Technol. Rev.* **2016**, *9*, 66–71. [CrossRef]
3. Emmanouloudis, D.; Garcia Rodriguez, J.L.; Zaimes, G.N.; Gimenez Suarez, M.C.; Filippidis, E. Euro-Mediterranean torrents: Case studies on tools that can improve their management. In *Mountain Ecosystems: Dynamics, Management and Conservation*; Richards, K.E., Ed.; Nova Science Publishers: Hauppauge, NY, USA, 2011; pp. 1–44.
4. Saleh, A.S.; AI-Hatrushi, S.M. Torrential flood hazards assessment, management, and mitigation, in Wadi Aday, Muscat Area, Sultanate of Oman, a GIS and RS approach. *Egypt. J. Remote Sens. Space Sci.* **2009**, *12*, 71–86.

5. Gaume, E.; Bain, V.; Bernardara, P.; Newinger, O.; Barbuc, M.; Bateman, A.; Blaškovičová, L.; Blöschl, G.; Borga, M.; Dumitrescu, A.; et al. A compilation of data on European flash floods. *J. Hydrol.* **2009**, *367*, 70–78. [CrossRef]
6. Bouadila, A.; Tzoraki, O.; Benaabidate, L. Hydrological modeling of three rivers under Mediterranean climate in Chile, Greece, and Morocco: Study of high flow trends by indicator calculation. *Arab. J. Geosci.* **2020**, *13*, 1–17. [CrossRef]
7. Kundzewicz, Z.W.; Kanae, S.; Seneviratne, S.I.; Handmer, J.; Nicholls, N.; Peduzzi, P.; Mechler, R.; Bouwer, L.; Arnell, N.; Mach, K.; et al. Flood risk and climate change: Global and regional perspectives. *Hydrol. Sci. J.* **2014**, *59*, 1–28. [CrossRef]
8. Gaume, E.; Borga, M.; Llassat, M.C.; Maouche, S.; Lang, M.; Diakakis, M. Mediterranean extreme floods and flash floods. In *The Mediterranean Region under Climate Change. A Scientific Update*; Thiébault, S., Moatti, J.-P., Eds.; IRD Editions. Coll. Synthèses: Marseille, France, 2016; pp. 133–144.
9. Rault, P.A.; Koundouri, P.; Akinsete, E.; Ludwig, R.; Huber-Garcia, V.; Tsani, S.; Acuna, V.; Kalogianni, E.; Luttik, J.; Kokg, K.; et al. Down scaling of climate change scenarii to river basin level: A transdisciplinary methodology applied to Evrotas river basin, Greece. *Sci. Total Environ.* **2019**, *660*, 1623–1632. [CrossRef]
10. Zaimes, G.N. Mediterranean Riparian Areas—Climate change implications and recommendations. *J. Environ. Biol.* **2020**, *41*, 957–965. [CrossRef]
11. Calbo, J. Possible climate change scenarios with specific reference to Mediterranean regions. In *Water Scarcity in the Mediterranean*; Sabater, S., Barceló, D., Eds.; Springer: Berlin, Germany, 2010; pp. 1–13.
12. Fyllas, N.M.; Christopoulou, A.; Galanidis, A.; Michelaki, C.Z.; Giannakopoulos, C.; Dimitrakopoulos, P.G.; Arianoutsou, M.; Gloor, M. Predicting species dominance shifts across elevation gradients in mountain forests in Greece under a warmer and drier climate. *Reg. Environ. Chang.* **2017**, *17*, 1165–1177. [CrossRef]
13. Molnar, P. Climate change, flooding in arid environments, and erosion rates. *Geology* **2001**, *29*, 1071–1074. [CrossRef]
14. Gasith, A.; Resh, V.H. Streams in Mediterranean climate regions: Abiotic influences and biotic responses to predictable seasonal events. *Annu. Rev. Ecol. Evol. Syst.* **1999**, *30*, 51–81. [CrossRef]
15. Peña-Angulo, D.; Nadal-Romero, E.; González-Hidalgo, J.C.; Albaladejo, J.; Andreu, V.; Barhi, H.; Bernal, S.; Biddoccu, M.; Bienes, R.; Campo, J.; et al. Relationship of weather types on the seasonal and spatial variability of rainfall, runoff, and sediment yield in the western Mediterranean basin. *Atmosphere* **2020**, *11*, 609. [CrossRef]
16. Rodrigo-Comino, J.; Senciales, J.M.; Sillero-Medina, J.A.; Gyasi-Agyei, Y.; Ruiz-Sinoga, J.D.; Ries, J.B. Analysis of weather-type-induced soil erosion in cultivated and poorly managed abandoned sloping vineyards in the Axarquía Region (Málaga, Spain). *Air Soil Water Res.* **2019**, *12*, 1–11. [CrossRef]
17. Midgley, T.L.; Fox, G.A.; Derek, M.; Heeren, D.M. Evaluation of the bank stability and toe erosion model (BSTEM) for predicting lateral retreat on composite streambanks. *Geomorphology* **2012**, *145-146*, 107–144. [CrossRef]
18. Pierzynski, G.M.; Sims, J.T.; Vance, G.F. *Soils and Environmental Quality*; CRC Press: Boca Raton, FL, USA, 2000.
19. Diakakis, M.; Mavroulis, S.; Deligiannakis, G. Floods in Greece, a statistical and spatial approach. *Nat. Hazards* **2012**, *62*, 485–500. [CrossRef]
20. Giannaros, C.; Kotroni, V.; Lagouvardos, K.; Oikonomou, C.; Haralambous, H.; Papagiannaki, K. Hydrometeorological and socio-economic impact assessment of stream flooding in southeast Mediterranean: The case of Rafina catchment (Attica, Greece). *Water* **2020**, *12*, 2426. [CrossRef]
21. Polinesi, G.; Recchioni, C.; Turco, R.; Salvati, L.; Rontos, K.; Comino, J.R.; Benassi, F. Population trends and urbanization: Simulating density effects using a local regression approach. *ISPRS Int. J. Geo Inf.* **2020**, *9*, 454. [CrossRef]
22. Borga, M.; Stoffel, M.; Marchi, L.; Marra, F.; Jakob, M. Hydrogeomorphic response to extreme rainfall in headwater systems: Flash floods and debris flows. *J. Hydrol.* **2014**, *518*, 194–205. [CrossRef]
23. Steiger, J.; Gurnell, A.M. Spatial hydrogeomorphological influences on sediment and nutrient deposition in riparian zones: Observations from the Garonne River, France. *Geomorphology* **2003**, *49*, 1–23. [CrossRef]
24. Cooper, J.R.; Gilliam, J.W.; Daniels, R.B.; Robarge, W.P. Riparian areas as filters for agricultural sediment. *Soil Sci. Soc. Am. J.* **1987**, *51*, 416–420. [CrossRef]

25. Zaimes, G.N.; Iakovoglou, V.; Emmanouloudis, D.; Gounaridis, D. Riparian areas of Greece: Their definition and characteristics. *J. Eng. Sci. Technol. Rev.* **2010**, *3*, 176–183. [CrossRef]
26. Schultz, R.C.; Collettil, J.P.; Isenhart, T.M.; Simpkins, W.W.; Mize, C.W.; Thompson, M.L. Design and placement of a multi-species riparian buffer strip system. *Agrofor. Syst.* **1995**, *29*, 201–226. [CrossRef]
27. Iakovoglou, V.; Zaimes, G.N.; Gounaridis, D. Riparian areas in urban settings: Two case studies from Greece. *Int. J. Innov. Sustain. Dev.* **2013**, *7*, 271–288. [CrossRef]
28. Saint-Laurent, D.; Arsenault-Boucher, L.; Berthelot, J.S. Contrasting effects of flood disturbance on alluvial soils and riparian tree structure and species composition in mixed temperate forests. *Air Soil Water Res.* **2019**, *12*, 1–11. [CrossRef]
29. Hefting, M.M.; Clement, J.C.; Bienkowski, P.; Dowrick, D.; Guenat, C.; Butturini, A.; Topa, S.; Pinay, G.; Verhoeven, J.T. The role of vegetation and litter in the nitrogen dynamics of riparian buffer zones in Europe. *Ecol. Eng.* **2005**, *24*, 465–482. [CrossRef]
30. Zaimes, G.N.; Schultz, R.C. Riparian land-use impacts on bank erosion and deposition of an incised stream in north-central Iowa, USA. *Catena* **2015**, *125*, 61–73. [CrossRef]
31. Naiman, R.J.; Decamps, H.; Pollock, M. The role of riparian corridors in maintaining regional biodiversity. *Ecol. Appl.* **1993**, *3*, 209–212. [CrossRef]
32. Piégay, H.; Gurnell, A.M. Large woody debris and river geomorphological pattern: Examples from SE France and S. England. *Geomorphology* **1997**, *19*, 99–116. [CrossRef]
33. Jeffries, R.; Darby, S.E.; Sear, D.A. The influence of vegetation and organic debris on flood-plain sediment dynamics: Case study of a low-order stream in the New Forest, England. *Geomorphology* **2003**, *51*, 61–80. [CrossRef]
34. Wilford, D.J.; Sakals, M.E.; Innes, J.L.; Sidle, R.C.; Bergerud, W.A. Recognition of debris flow, debris flood and flood hazard through watershed morphometrics. *Landslides* **2004**, *1*, 61–66. [CrossRef]
35. Church, M.; Jakob, M. What is a debris flood? *Water Resour. Res.* **2020**, *56*, e2020WR027144. [CrossRef]
36. Koutalakis, P.; Zaimes, G.N.; Iakovoglou, V.; Ioannou, K. Reviewing soil erosion in Greece. *Ital. J. Eng. Geol. Environ.* **2015**, *9*, 936–941.
37. Margaroni, S.G.; Tzoraki, O.; Velegrakis, A. Soil erosion risk of Lesvos Island. In Proceedings of the 11th Panhellenic Symposium on Oceanography & Fisheries, Mytilene, Lesvos, Greece, 13–17 May 2015.
38. Myronidis, D.I.; Emmanouloudis, D.A.; Mitsopoulos, I.A.; Riggos, E.E. Soil erosion potential after fire and rehabilitation treatments in Greece. *Environ. Model. Assess.* **2010**, *15*, 239–250. [CrossRef]
39. Anache, J.A.; Wendland, E.C.; Oliveira, P.T.; Flanagan, D.C.; Nearing, M.A. Runoff and soil erosion plot-scale studies under natural rainfall: A meta-analysis of the Brazilian experience. *Catena* **2017**, *152*, 29–39. [CrossRef]
40. Moraetis, D.; Efstathiou, D.; Stamati, F.; Tzoraki, O.; Nikolaidis, N.P.; Schnoor, J.L.; Vozinakis, K. High-frequency monitoring for the identification of hydrological and bio-geochemical processes in a Mediterranean river basin. *J. Hydrol.* **2010**, *389*, 127–136. [CrossRef]
41. King, C.; Baghdadi, N.; Lecomte, V.; Cerdan, O. The application of remote-sensing data to monitoring and modelling of soil erosion. *Catena* **2005**, *62*, 79–93. [CrossRef]
42. Pérez, E.; García, P. Monitoring soil erosion by raster images: From aerial photographs to drone taken pictures. *Eur. J. Geogr.* **2017**, *8*, 116–128.
43. Koutalakis, P.; Tzoraki, O.; Zaimes, G.N. Detecting riverbank changes with remote sensing tools. Case study: Aggitis River in Greece. *An. Univ. Dunărea de Jos Galați Fasc. II Mat. Fiz. Mec. Teor./Ann. Dunarea de Jos Univ. Galati Fascicle II Math. Phys. Theor. Mech.* **2019**, *42*, 134–142. [CrossRef]
44. Restas, A. Drone applications for supporting disaster management. *World J. Eng. Technol.* **2015**, *3*, 316. [CrossRef]
45. Erdelj, M.; Natalizio, E.; Chowdhury, K.R.; Akyildiz, I.F. Help from the sky: Leveraging UAVs for disaster management. *IEEE Pervasive Comput.* **2017**, *16*, 24–32. [CrossRef]
46. Şerban, G.; Rus, I.; Vele, D.; Breţcan, P.; Alexe, M.; Petrea, D. Flood-prone area delimitation using UAV technology, in the areas hard-to-reach for classic aircrafts: Case study in the north-east of Apuseni Mountains, Transylvania. *Nat. Hazards* **2016**, *82*, 1817–1832. [CrossRef]
47. Niethammer, U.; James, M.R.; Rothmund, S.; Travelletti, J.; Joswig, M. UAV-based remote sensing of the Super-Sauze landslide: Evaluation and results. *Eng. Geol.* **2012**, *128*, 2–11. [CrossRef]
48. Koutalakis, P.; Tzoraki, O.; Zaimes, G. UAVs for hydrologic scopes: Application of a low-cost UAV to estimate surface water velocity by using three different image-based methods. *Drones* **2019**, *3*, 14. [CrossRef]

49. Lou, H.; Wang, P.; Yang, S.; Hao, F.; Ren, X.; Wang, Y.; Shi, L.; Wang, J.; Gong, T. Combining and comparing an unmanned aerial vehicle and multiple remote sensing satellites to calculate long-term river discharge in an ungauged water source region on the Tibetan Plateau. *Remote Sens.* **2020**, *12*, 2155. [CrossRef]
50. Yang, S.; Wang, P.; Lou, H.; Wang, J.; Zhao, C.; Gong, T. Estimating river discharges in ungauged catchments using the slope–area method and unmanned aerial vehicle. *Water* **2019**, *11*, 2361. [CrossRef]
51. Zwęgliński, T. The use of drones in disaster aerial needs reconnaissance and damage assessment—Three-dimensional modeling and orthophoto map study. *Sustainability* **2020**, *12*, 6080. [CrossRef]
52. Borg Galea, A.; Sadler, J.P.; Hannah, D.M.; Datry, T.; Dugdale, S.J. Mediterranean intermittent rivers and ephemeral streams: Challenges in monitoring complexity. *Ecohydrology* **2019**, *12*, e2149. [CrossRef]
53. Georgi, J.N.; Sarikou, S. Unification and planning of urban public spaces in Drama, Greece with bioclimatic criteria. In Proceedings of the 46th Congress of the European Regional Science Association (ERSA) "Enlargement, Southern Europe and the Mediterranean", Volos, Greece, 30 August–3 September 2006.
54. Kirkenidis, C.; Kirkenidis, I.; Stefanidis, P. Orhtological management of hydrological runoff basins of the prefecture of drama (current situation-protective actions-perspectives). In Proceedings of the 5th International Conference on Information and Communication Technologies for Sustainable Agri-production and Environment (HAICTA 2011), Skiathos, Greece, 8–11 September 2011.
55. Ananiadou-Tzimopoulou, M.; Fatouros, D.A. The Ayia Varvara site project: A case of urban landscape design. *Landsc. Urban Plan.* **1990**, *19*, 69–97. [CrossRef]
56. Frisi, P. *A Treatise on Rivers and Torrents: With the Method of Regulating Their Course and Channels*; Longman, Hurst, Rees, Orme, and Brown: London, UK, 1861; pp. 1728–1784.
57. Numbere, A.O.; Maimaitijiang, M. Mapping of Nypa palm invasion of mangrove forest using low cost and high resolution UAV digital imagery in the Niger Delta Nigeria. *Curr. Trends For. Res.* **2019**. [CrossRef]
58. Carnevali, L.; Ippoliti, E.; Lanfranchi, F.; Menconero, S.; Russo, M.; Russo, V. Close-range mini-UAVS photogrammetry for architecture survey. *Int. Arch. Photogramm. Remote Sens. Spat. Inf. Sci.* **2018**, *42*, 2. [CrossRef]
59. James, M.R.; Robson, S.; d'Oleire-Oltmanns, S.; Niethammer, U. Optimising UAV topographic surveys processed with structure-from-motion: Ground control quality, quantity and bundle adjustment. *Geomorphology* **2017**, *280*, 51–66. [CrossRef]
60. Stott, E.; Williams, R.D.; Hoey, T.B. Ground control point distribution for accurate kilometre-scale topographic mapping using an RTK-GNSS unmanned aerial vehicle and SfM photogrammetry. *Drones* **2020**, *4*, 55. [CrossRef]
61. Laporte-Fauret, Q.; Marieu, V.; Castelle, B.; Michalet, R.; Bujan, S.; Rosebery, D. Low-cost UAV for high-resolution and large-scale coastal dune change monitoring using photogrammetry. *J. Mar. Sci. Eng.* **2019**, *7*, 63. [CrossRef]
62. Themistocleous, K.; Agapiou, A.; King, H.M.; King, N.; Hadjimitsis, D.G. More than a flight: The extensive contributions of UAV flights to archaeological research–the case study of curium site in Cyprus. In *Digital Heritage. Progress in Cultural Heritage: Documentation, Preservation, and Protection, Proceedings of the Euro-Mediterranean Conference EuroMed 2014, Cham, Switzerland, 3–8 November 2014*; Springer: Cham, Switzerland, 2014.
63. Jebur, A.; Abed, F.; Mohammed, M. Assessing the performance of commercial Agisoft PhotoScan software to deliver reliable data for accurate3D modelling. In Proceedings of the 3rd International Conference on Buildings, Construction and Environmental Engineering, BCEE3-2017, Sharm el-Shiekh, Egypt, 23–25 October 2017; MATEC Web of Conferences, EDP Sciences: Les Ulis, France, 2018; Volume 162, p. 11.
64. Turner, D.; Lucieer, A.; Wallace, L. Direct georeferencing of ultrahigh-resolution UAV imagery. *IEEE Trans. Geosci. Remote Sens.* **2013**, *52*, 2738–2745. [CrossRef]
65. Bjorkland, R.; Pringle, M.C.; Newton, B. A stream visual assessment protocol (SVAP) for riparian landowners. *Environ. Monit. Assess.* **2001**, *68*, 99–125. [CrossRef] [PubMed]
66. Vlami, V.; Zogaris, S.; Djuma, H.; Kokkoris, I.P.; Kehayias, G.; Dimopoulos, P. A field method for landscape conservation surveying: The landscape assessment protocol (LAP). *Sustainability* **2019**, *11*, 2019. [CrossRef]
67. USDA-NRCS. *Stream Visual Assessment Protocol Version 2, National Biology Handbook Subpart B—Conservation Planning*; United States Department of Agriculture, Natural Resources Conservation Service: Portland, OR, USA, 2009; Part 614; p. 75.

68. Gkiatas, G.; Pagonis, G.; Iakovoglou, V.; Raptis, D.; Emmanouloudis, D.; Zaimes, G.N. Assessing rural and agricultural riparian areas of Greece with the use of GIS and SVAP. In Proceedings of the Natural Resources, Green Technology and Sustainable Development-GREEN/2, Zagreb, Croatia, 5–7 October 2016; Croatian Forest Research Institute, University of Zagreb, Institute for Adriatic Crops and Karst Reclamation, Croatian Society of Biotechnology, Academy of Forestry Sciences: Zagreb, Croatia, 2016.
69. Zaimes, G.N.; Iakovoglou, V.; Koutalakis, P.; Kiosses, V.; Giatas, G.; Savvopoulou, A. Riparian areas as a tool to mitigate climate change impacts in urban settings: The case study of Drama City, Greece. In Proceedings of the International Conference on Climate Change and Forestry, Antalya, Turkey, 13–14 November 2019; Atvin Coruh University: Artvin, Turkey, 2019.
70. Iakovoglou, V.; Koutsoumis, A.; Zaimes, G.N.; Emmanouloudis, D. Using the Stream Visual Assessment Protocol (SVAP) to evaluate the streams and their riparian areas of the Volvi Lake watershed in Greece. In Proceedings of the International Caucasia Forestry Symposium, Artvin, Turkey, 24–26 October 2013; Atvin Coruh University: Artvin, Turkey, 2013.
71. Sauquet, E.; van Meerveld, I.; Sefton, C.; Gallart, F.; Laaha, G.; Bezdan, A.; Banasik, K.; De Girolamo, A.M.; Gauster, T.; Karagiozova, T.; et al. *A Catalogue of European Intermittent Rivers and Ephemeral Streams*; Technical report SMIRES COST Action CA15113; HAL Archives ouvertes, Centre pour la Communication Scientifique Directe (CCSD): Lyon, France, 2019; p. 100, hal-02914572.
72. Tzoraki, O.; Nikolaidis, N.P.; Amaxidis, Y.; Skoulikidis, N.T. In-stream biogeochemical processes of a temporary river. *Environ. Sci. Technol.* **2007**, *41*, 1225–1231. [CrossRef]
73. Gallart, F.; Prat, N.; García-Roger, E.M.; Latron, J.; Rieradevall, M.; Llorens, P.; Barberá, G.G.; Brito, D.; De Girolamo, A.M.; Lo Porto, A.; et al. A novel approach to analysing the regimes of temporary streams in relation to their controls on the composition and structure of aquatic biota. *Hydrol. Earth Syst. Sci.* **2012**, *16*, 3165–3182. [CrossRef]
74. Tzoraki, O. Operating small hydropower plants in Greece under intermittent flow uncertainty: The case of Tsiknias River (Lesvos). *Challenges* **2020**, *11*, 17. [CrossRef]
75. Stavropoulos, S.; Zaimes, G.N.; Filippidis, E.; Diaconu, D.C.; Emmanouloudis, D. Mitigating flash floods with the use of new technologies: A multi-riteria decision analysis to map flood susceptibility for Zakynthos Island, Greece. *J. Urban Reg. Anal.* **2020**, *12*, 233–248. [CrossRef]
76. Eisenbeiss, H.; Sauerbier, M. Investigation of UAV systems and flight modes for photogrammetric applications. *Photogramm. Rec.* **2011**, *26*, 400–421. [CrossRef]
77. Fernández-Hernandez, J.; González-Aguilera, D.; Rodríguez-Gonzálvez, P.; Mancera-Taboada, J. Image-based modelling from unmanned aerial vehicle (UAV) photogrammetry: An effective, low-cost tool for archaeological applications. *Archaeometry* **2015**, *57*, 128–145. [CrossRef]
78. Sanhueza, D.; Picco, L.; Ruiz-Villanueva, V.; Iroumé, A.; Ulloa, H.; Barrientos, G. Quantification of fluvial wood using UAVs and structure from motion. *Geomorphology* **2019**, *345*, 106837. [CrossRef]
79. Seier, G.; Schöttl, S.; Kellerer-Pirklbauer, A.; Glück, R.; Lieb, G.K.; Hofstadler, D.N.; Sulzer, W. Riverine sediment changes and channel pattern of a gravel-bed mountain torrent. *Remote Sens.* **2020**, *12*, 3065. [CrossRef]
80. Arthun, D.; Zaimes, G.N. Channel changes following human activity exclusion in the riparian areas of Bonita Creek, Arizona, USA. *Landsc. Ecol. Eng.* **2020**, *16*, 263–271. [CrossRef]
81. Florsheim, J.L.; Mount, J.F. Restoration of floodplain topography by sand-splay complex formation in response to intentional levee breaches, Lower Cosumnes River, California. *Geomorphology* **2002**, *44*, 67–94. [CrossRef]
82. Nanson, G.C.; Croke, J.C. A genetic classification of floodplains. *Geomorphology* **1992**, *4*, 459–486. [CrossRef]
83. Baek, K.O.; Do Kim, Y. A case study for optimal position of fishway at low-head obstructions in tributaries of Han River in Korea. *Ecol. Eng.* **2014**, *64*, 222–230. [CrossRef]
84. Wu, C.Y.; Mossa, J. Decadal-scale variations of thalweg morphology and riffle–pool sequences in response to flow regulation in the lowermost Mississippi River. *Water* **2019**, *11*, 1175. [CrossRef]
85. Ilhardt, B.L.; Verry, E.S.; Palik, B.J. Defining riparian areas. Forestry and the riparian zone. In Proceedings of the Conference "Forestry and the Riparian Zone", Orono, ME, USA, 26 October 2000.
86. Bren, L.J. Riparian zone, stream, and floodplain issues: A review. *J. Hydrol.* **1993**, *150*, 277–299. [CrossRef]
87. Langhammer, J.; Vacková, T. Detection and mapping of the geomorphic effects of flooding using UAV photogrammetry. *Pure Appl. Geophys.* **2018**, *175*, 3223–3245. [CrossRef]

88. Langhammer, J.; Lendzioch, T.; Miřijovský, J.; Hartvich, F. UAV-based optical granulometry as tool for detecting changes in structure of flood depositions. *Remote Sens.* **2017**, *9*, 240. [CrossRef]
89. Woodget, A.S.; Austrums, R. Subaerial gravel size measurement using topographic data derived from a UAV-SfM approach. *Earth Surf. Process. Landf.* **2017**, *42*, 1434–1443. [CrossRef]
90. Switzer, A.D. Measuring and analyzing particle size in a geomorphic context. In *Treatise on Geomorphology*; Switzer, A., Kennedy, D.M., Eds.; Academic Press: San Diego, CA, USA, 2013; Volume 14, pp. 224–242.
91. Uysal, M.; Toprak, A.S.; Polat, N. DEM generation with UAV Photogrammetry and accuracy analysis in Sahitler hill. *Measurement* **2015**, *73*, 539–543. [CrossRef]
92. Chang, K.T.; Tsai, B.W. The effect of DEM resolution on slope and aspect mapping. *Cartogr. Geogr. Inf. Syst.* **1991**, *18*, 69–77. [CrossRef]
93. Li, J.; Wong, D.W. Effects of DEM sources on hydrologic applications. *Comput. Environ. Urban Syst.* **2010**, *34*, 251–261. [CrossRef]
94. Zaimes, G.N.; Tardio, G.; Iakovoglou, V.; Gimenez, M.; Garcia-Rodriguez, J.L.; Sangalli, P. New tools and approaches to promote soil and water bioengineering in the Mediterranean. *Sci. Total Environ.* **2019**, *693*, 133677. [CrossRef]